EXPERIMENT ALICE AT THE LHC

PNPI participants of the ALICE Collaboration: V.M. Samsonov, V.A. Guzey, V.S. Ivanov, E.L. Kryshen, A.V. Khanzadeev, M.V. Malaev, V.N. Nikulin, V.G. Ryabov, Yu.G. Ryabov, M.B. Zhalov

1. Introduction

Last decades, a study of one of the most exciting problems of high energy physics – properties of the extreme state of the nuclear matter created in collisions of ultrarelativistic heavy ions – were on the top of priority at the Relativistic Heavy Ion Collider (RHIC) at Brookhaven at the energy of colliding nuclei $s_{NN}^{1/2}$ = 200 GeV. A huge bulk of data was accumulated and processed by joint efforts of four collaborations (STAR, PHENIX, BRAHMS and PHOBOS). This allowed one to investigate a wide spectrum of observables in heavy ion collisions ranging from the global characteristics like multiplicity distributions of the produced particles and ratios of their integral yields to detailed studies of the Hanbury – Brown – Twiss (HBT) correlations, elliptic flows of different particles, and quenching of jets escaping from the hot medium produced in the central collisions. From a combined analysis of all these results it was stated that the hot gluon dominated medium was formed in the volume of about 150 fm^3 in collisions of ultrarelativistic heavy ions at $s_{NN}^{1/2}$ = 200 GeV. Even within the conservative estimates, this medium is characterized by the energy density of more than 5 GeV/fm^3, and by the lifetime of the order of 6 fm/c. Contrary to the QCD based expectations to find at high temperature a deconfined gas of weakly interactive quarks and gluons (Qaurk-Gluon Plasma), the medium created at RHIC appeared to resemble almost perfect parton liquid with very low shear viscosity. This exciting observation was mainly validated by three cornerstone phenomena discovered at RHIC: a large elliptic flow of the produced particles which was found to be close to the hydrodynamic limit of the ideal liquid, quark number scaling properties of the flowing particles at small transverse momenta, and strong quenching of jets due to the parton energy loss in the deconfined colour medium created in the central zone of ion interactions. So, before the start of the heavy ion program at the Large Hadron Collider (LHC) in 2010, the top priority question was how the properties of the medium created in the central collisions can change when the energy of the colliding ions is increased up to 1380 GeV/N, which is higher by more than one order in comparison to the energy 100 GeV/N of beams at RHIC. The ALICE detector [1] was designed and built to answer this question.

2. The ALICE detector

To perform a detailed study of the properties of the extreme state of the nuclear matter created in collisions of ultrarelativistic heavy ions at the LHC, the ALICE detector comprises a number of dedicated subsystems (Fig. 1).

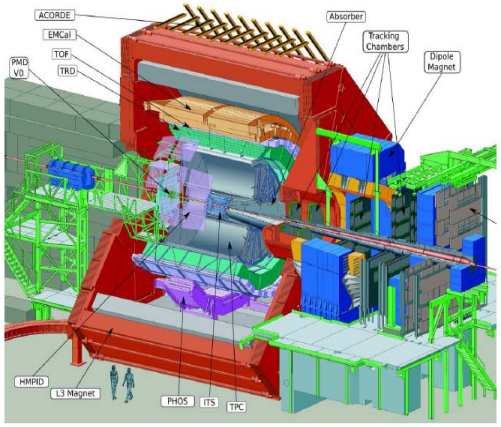

Fig. 1. Layout of the ALICE detector

Central barrel subdetectors – an Inner Tracking System (ITS), a Time Projection Chamber (TPC), a Transition Radiation Detector (TRD), and a Time-of-Flight (TOF) detector – cover the full azimuthal angle range at midrapidities $|\eta| < 0.9$. The calorimeters EmCal and PHOS have partial coverage at midrapidities. V0 detectors from both sides measure the charged particle multiplicity in the forward and backward directions at $-3.7 < \eta < -1.7$ and $2.8 < \eta < 5.1$ and are also used for triggering and centrality determination. Two Zero Degree Calorimeters are placed at a distance of about 114 m from the interaction zone to measure neutral particles, mainly neutrons.

The PNPI team in ALICE is responsible for the Muon Spectrometer system, which is placed in the forward direction and measures yields of muons from decays of the produced particles. The layout of the ALICE Muon spectrometer is shown in Fig. 2. The detector consists of an absorber, five tracking stations (ST1–ST5), two Trigger Stations (TS1 and TS2), a dipole magnet, and an iron wall. The selection of muons is based on their high penetrating power: most of particles other than muons are stopped inside the 4.3 m long composite absorber ($X_0 \approx 60$, $\lambda_{int} \approx 10$). The passed through particles are bent by the magnetic field of the dipole magnet. The tracking stations measure the particle track deviation: ST1 and ST2 measure the input angle, ST4 and ST5 measure the output direction, and ST3 gives track coordinates inside the dipole magnet. The dipole magnet (3 Tm field integral) is used for a momentum analysis. The iron wall located between the tracking and trigger parts of the detector makes an additional cleanup from non-muon components. The trigger Resistive Plate Chambers (RPCs) provide the tracklet information, thus one can easily estimate the transverse momentum of the particle. The trigger electronics performs an analysis of the data, and within 800 ns produces a trigger signal taking into account the threshold on the transverse momentum (1 GeV/c to select J/ψ and 5 GeV/c to select Υ).

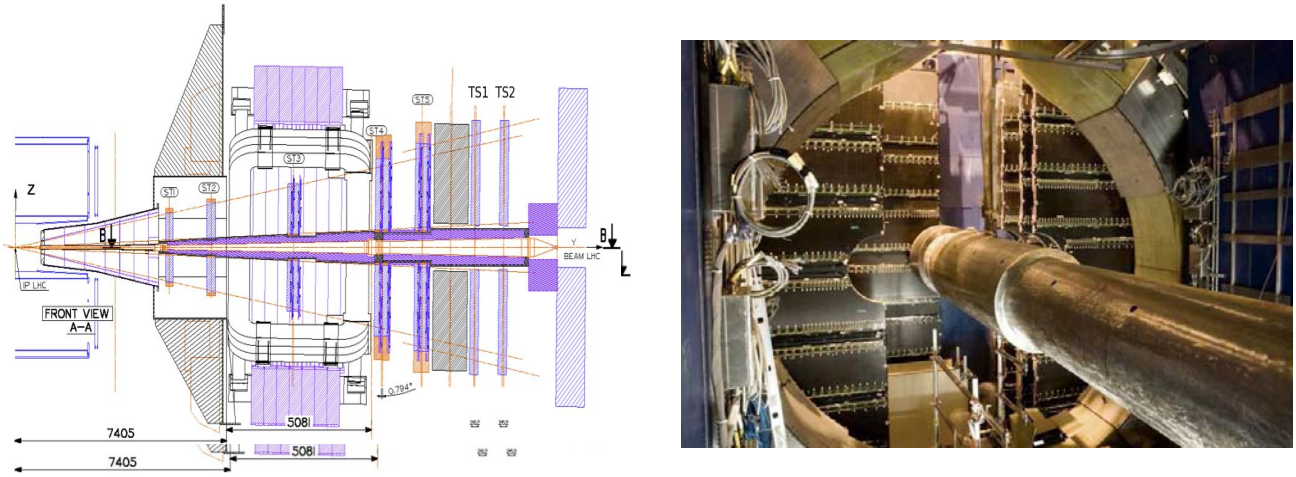

Fig. 2. Muon spectrometer longitudinal section and the layout of stations 3 and 4 (slat design) and the beam-shield tube

Large (up to 6 m), high granularity (capable to detect several hundred hits per plane per event), high resolution (better than 100 microns in the bending plane) detectors were built. The PNPI team participation in the Muon spectrometer hardware can be summarized as follows:

(i) Designing and building prototypes: the conception of the slat chambers (a plane composed of long rectangular detector elements was proposed by the PNPI team). The chamber prototypes were successfully tested at the CERN PS beam.

(ii) Manufacturing: a quarter of the tracking modules for ST3, ST4 and ST5 were assembled at PNPI. The PNPI team also built the tooling for production of the modules (machines for high precision trimming of the printed circuit boards for Cagliari and Kolkata, a wire stress measurement device, a radioactive source scanning system, a HV test-bench).

(iii) Commissioning and maintenance: participation in the final tests and chamber assembly at CERN, installation of the chambers in the cave, elimination of the electronic noise, repairing of faulty components during technical stops, participation in shifts at the expert level.

Segmented cathode pad chambers with about 1.09 millions readout channels were used in order to achieve the required performance. The on-board signal encoding and zero suppression enable a fast readout procedure. Up to 1200 channels are daisy-chained and organized in data buses, which come to the readout system. The readout crate can read up to 50 data buses at a rate up to 1 kHz. The system includes 20 crates. In order to align the tracking modules, their positions in the first approximation were measured by means of the photogrammetry method (a PNPI representative participated in the ALICE survey group). The final alignment procedure was done using particle tracks in the absence of the magnetic field. Simulations have shown that the mass resolution of about 75 MeV/c^2 for J/ψ and about 150 MeV/c^2 for Υ can be achieved.

3. Upgrade plans

The LHC has recently entered a two-year period of Long Shutdown 1 dedicated to increasing the energy of the accelerated particles to the designed value of 7 TeV per beam. ALICE will take this opportunity to complete the approved detector design and consolidate the detector performance. In 2015–2017, ALICE is going to fulfill the initially approved plans and to collect about 1 nb^{-1} of Pb-Pb data at the full LHC energy. This data taking period will be followed by Long Shutdown 2 aimed to upgrade the LHC luminosity capabilities by a factor of 10 and, hence, to reach the Pb-Pb interaction rates of about 50 kHz.

ALICE is going to take full advantage of the high-luminosity LHC [2]. The intent is to explore 10^{10} minimum bias events, a factor of 100 more than it was planned before the upgrade. This would allow one to perform multi-dimensional analyses of rare low-p_T observables (*e.g.*, charm baryons) with unprecedented statistical and systematic accuracy. This ambitious goal relies on the development of a new data acquisition system based on pipeline readout and a high-level trigger with online event reconstruction and selection. In addition, the readout electronics of all detector subsystems has to be upgraded, and new GEM-based readout chambers will be installed in TPC to meet the high rate requirements. Besides, in order to exploit low-p_T and charm physics, ALICE is going to install a smaller radius beam pipe and a new inner tracking system with a pipeline readout, the reduced material budget of only 0.3 % of the radiation length and smaller pixel sizes providing the hit resolution of the order of 4 μm and improving the vertexing precision by a factor of 3.

Another essential part of the upgrade project is the Muon Forward Tracker (MFT), a silicon pixel detector will be added in the Muon Spectrometer upstream of the hadron absorber [3]. The MFT will provide reliable measurements of the muon track offsets with respect to the primary vertex of the interaction and enhance the ALICE capabilities for detecting muons at the forward rapidity. The presence of the MFT detector will give an access to new observables like prompt/displaced J/ψ separation and charm/beauty separation, in both cases at very low transverse momentum.

The PNPI team actively participates in the upgrade activities, namely in the construction and integration of the MFT support structures and in the development of the new trigger system allowing one to combine old hardware triggers with the foreseen pipeline readout architecture.

4. Global observables from the first ALICE results on heavy ion collisions

During the 2010–2013 runs at proton-proton, ion-ion and ion-proton beams, a large volume of data was collected with general purpose triggers, and additionally some specialized hard interaction triggers were also used to study in more details specific processes with relatively small cross sections. The information on major data taking periods is shown in Table 1.

Table 1

Summary of the data sets recorded with ALICE [4]

System	$s_{NN}^{1/2}$, TeV	Year	Min. bias triggers, M	Int. luminosity
pp	7	2010	800	17 μb^{-1}
pp	7	2011	800	2 pb^{-1}
pp	2.76	2011	70	20 nb^{-1}
pp	8	2012	500	5 pb^{-1}
Pb-Pb	2.76	2011	30	4 μb^{-1}
Pb-Pb	2.76	2012	9	80 μb^{-1}
p-Pb	5.02	2013	140	12 μb^{-1}

Already the first result obtained and published by ALICE [5] after the run at $s_{NN}^{1/2}$ = 2.76 TeV/N in 2010 revealed a pronounced effect due to increasing the energy of collisions in comparison with the energies at RHIC. The charge particle multiplicity density measured in the central lead-lead collisions scaled by the number of the nucleon pairs participating in the collision appeared to rise steeper than the charge particle multiplicity density in *pp* interactions at the same energy (Fig. 3). From the HBT correlations of charged hadrons, the transverse radius of the produced medium was found to be $R_t \approx 6$ fm, the medium volume exceeding the RHIC value by a factor of about 1.5–2.

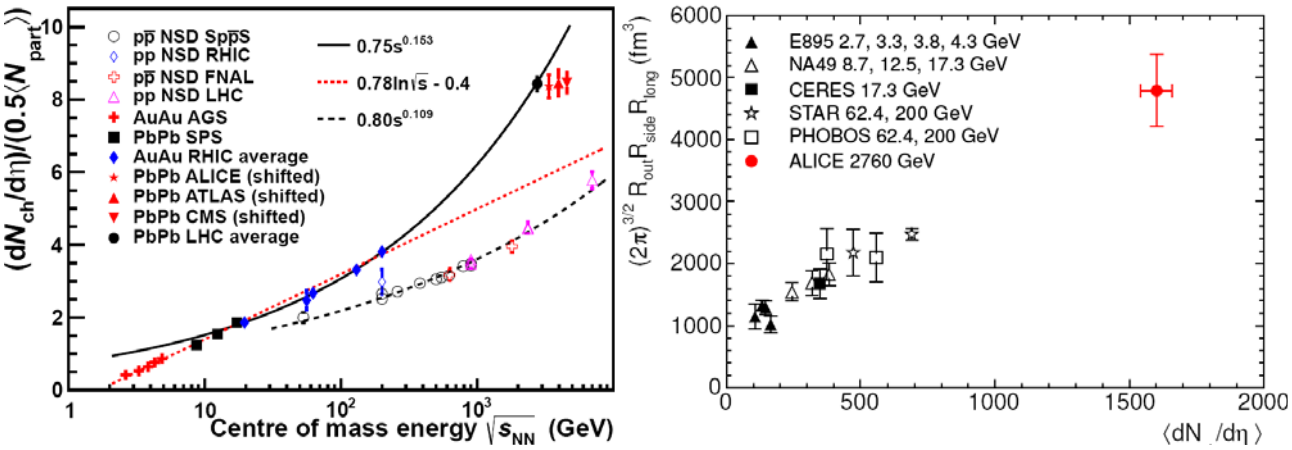

Fig. 3. Charged particle multiplicity density and the volume of the medium created in the central PbPb collisions measured in the ALICE experiment

The measured value $dN_{ch}/d\eta \approx 1600$ allowed one to estimate the energy density using as a guess the Bjorken model formula. Assuming the same formation time $\tau_{form} \approx 1$ fm/c at the RHIC and LHC energies, this leads to the value $\varepsilon \approx 15$ GeVfm^{-3}, exceeding the value found at RHIC at least by a factor of about 3. On the assumption of establishing the state of the thermodynamics equilibration, the corresponding increase of the temperature would be by 30 % above the RHIC value. One has to note that the same Bjorken formula gives an estimate of the energy density deposited during the time of the ion interaction ($\Delta\tau_{int} \approx 2R_A/\gamma_L \approx$ ≈ 0.01 fm/c) on the level of 1500 GeV/fm^3. This rises a question about the mechanism driving the equilibration of the created medium with so high initial energy density during a rather short time of the order of 1 fm/c.

A detailed analysis of the charged particle yields shows [6] that the developed elliptic flows at the LHC energies are close to that found at RHIC (Fig. 4). A slight increase of the parameter v_2 characterizing the elliptic flow is mainly due to an increase of the average transverse momentum of particles at the LHC energies. Note that in the case of formation of the weakly interactive Quark-Gluon Plasma (QGP) at the LHC one should expect a decrease of the elliptic flows.

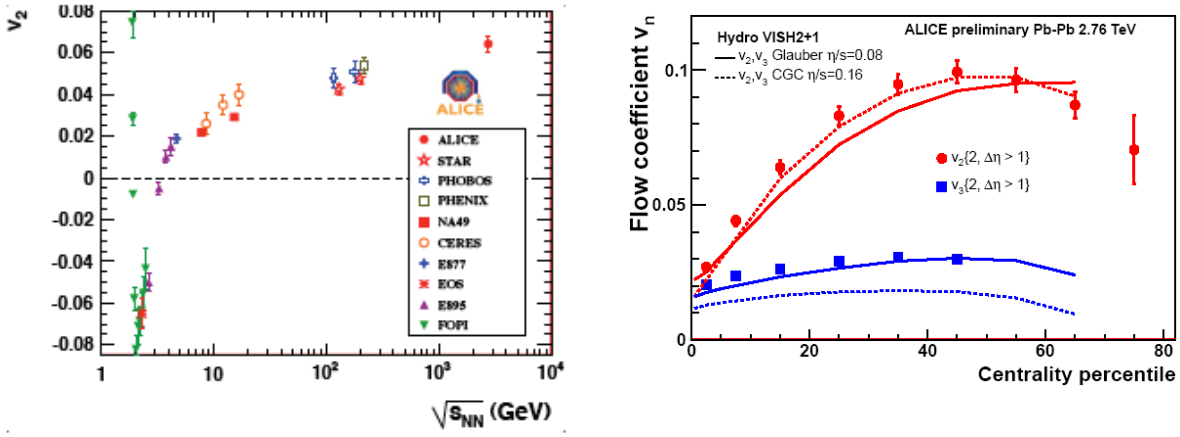

Fig. 4. Dependence of the integral elliptic flow coefficient on the energy (left), description of the measured by ALICE elliptic and triangular flow coefficients by the hydrodynamical model with different values of the shear viscosity (right)

In Fig. 4 (right side), it is seen that the elliptic flow coefficient can be reasonably described by hydrodynamics with a small ratio of shear viscosity to enthropy $\eta/s \approx 0.08$–0.16, close to the unitarity limit $\eta/s \approx 1/4\pi$ obtained for this ratio from the Anti-De-Sitter/Conformal-Field-Theory correspondence. This is a clear indication that the medium formed in Pb + Pb collisions at the LHC energies has the properties of

the almost perfect liquid. Even on the face of it, the behaviour of the elliptic flow coefficients for different hadrons at small transverse momenta (Fig. 5, left side) hints that the difference between the flowing of mesons and baryons can be removed if one takes into account that these hadrons comprise different numbers of the valence quarks. Indeed, after scaling of the value of these coefficients and transverse momenta of hadrons by the numbers of quarks (Fig. 5, right side), the partial coefficients become very similar, while, contrary to the picture found at RHIC, some difference still persists. Such scaling property means that the elliptic flow is mainly formed at the early stage of the expansion when the created medium is still in the partonic state. A more detailed analysis of the particle flows including studies of the hadrons comprising heavy quarks and the behaviour of the higher harmonics is under progress to get better understanding of the observed difference in the scaling properties and of the influence of fluctuations on the hydrodynamic properties of the created medium.

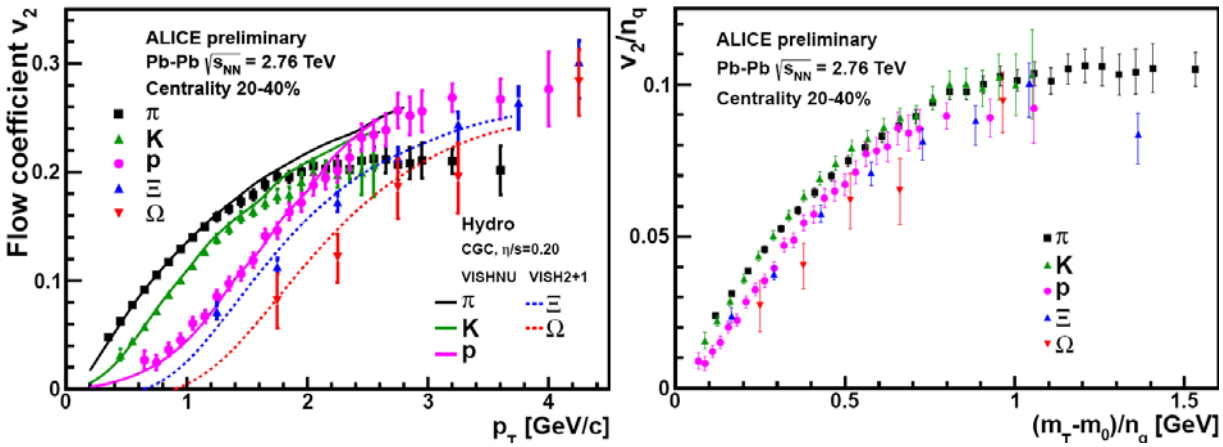

Fig. 5. Scaling of the elliptic flow coefficients for different hadrons by the number of quarks they are composed of

The third cornerstone phenomenon, jet quenching and parton recombination, is considered among the main signatures of the quark-gluon plasma. In ultrarelativistic heavy ion collisions they manifest themselves in suppression of high-p_T hadron production and in enhancement of baryon production at intermediate values of p_T. Experimental study of these effects is important for understanding and numerical estimation of the plasma transport properties and its time-spatial evolution.

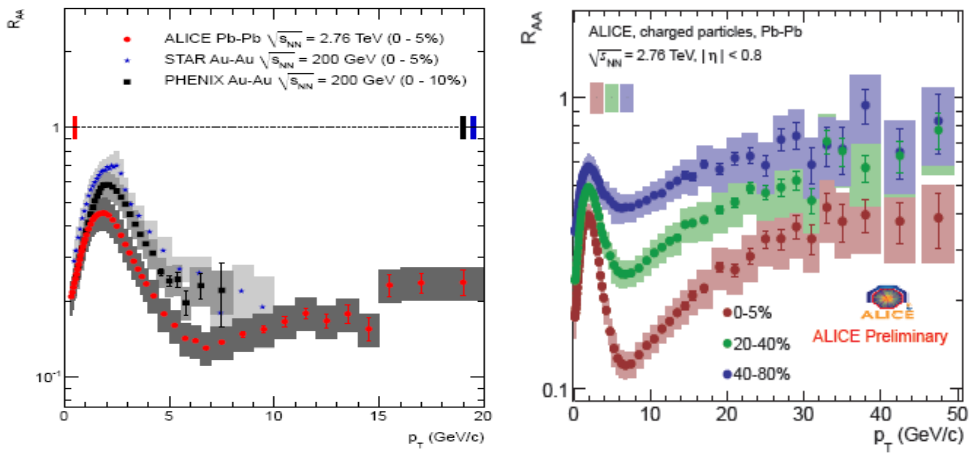

Fig. 6. Factor of nuclear modification of leading hadrons observed at ALICE in comparison with RHIC results

It is generally accepted to characterize the effect of jet quenching by the ratio R_{AA} of the leading hadron yield in nucleus-nucleus collision to that in proton-proton scaled by the number of the interacting nucleon pairs. From the analysis of the RHIC data it was found that three main phenomena can contribute to

the modification of the leading hadron yield in nucleus-nucleus collisions – Cronin effect, shadowing of the quark and gluons in the initial state, and the energy loss of fast partons crossing the created medium. However, a very strong suppression can be explained only if one takes into account the energy loss of the fast coloured parton which crosses the deconfined medium consisting of quarks and gluons. The nuclear modification factor measured with the ALICE detector [7] at the invariant energy 2.76 TeV is compared to that determined at RHIC energies, Fig. 6. Up to the transverse momenta of about 7 GeV/c, the results are in close agreement, thus confirming the strong jet quenching effect due to the parton energy losses in the coloured media at the energies of the LHC.

To achieve an unambiguous interpretation of the nuclear modification effects and to discriminate between theoretical models, one needs to measure production of identified hadrons containing light (u, d), strange (s) and heavy (c, b) quarks at intermediate and high transverse momenta.

5. Heavy quarks: hints of thermalization?

Charm quarks are abundantly produced at the LHC providing a powerful tool to study both the properties of the medium and the transport properties of the charm quarks. In-medium energy loss for heavy quarks is expected to be smaller than that for light quarks and gluons due to the colour charge and gluon-bremsstrahlung dead cone effects. Figure 7 (left) presents ALICE results [8] on the nuclear modification factors for D^0, D^+ and D^{*+} mesons. The observed suppression is similar for different meson species and reaches a factor of 5 at $p_T \sim 10$ GeV/c, being very close to the average charged particle suppression and providing an indication of no strong colour charge dependence of the in-medium energy loss. A similar suppression pattern was also observed in semi-leptonic decay channels of heavy flavours.

The observed elliptic flow of prompt D^0 mesons, shown in Fig. 7 (right), is also comparable with v_2 of light hadrons in favour of possible thermalization of charm quarks in the hot QCD medium created in heavy-ion collisions at the LHC.

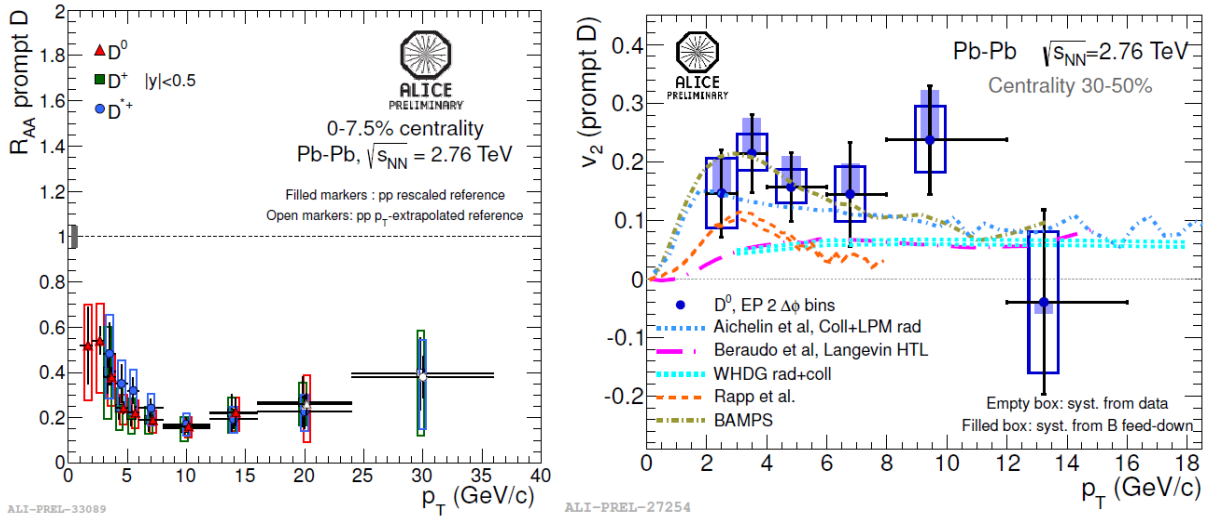

Fig. 7. Nuclear modification factors for D^0, D^+, and D^{*+} mesons in central Pb-Pb collisions (left) and v_2 for prompt D^0 mesons in 30–50 % centrality bin (right) as functions of p_T (from Ref. [8])

6. Charmonium: suppression or regeneration?

30 years ago, the charmonium suppression was proposed as the best signature of the deconfined phase since the deconfined hot medium prevents formation of bound $\overline{c}c$ states due to colour screening effects in the QGP. A large suppression was indeed observed at the SPS and RHIC. However, with high multiplicity of heavy quarks at the LHC, one should consider another scenario: an enhancement of the bound $\overline{c}c$ states *via* regeneration in the thermalized QGP medium or during hadronization.

The nuclear modification factor for J/ψ mesons measured by ALICE at the forward rapidity is shown in Fig. 8 (left) as a function of the number of participants $\langle N_{part} \rangle$ [9]. The observed suppression flattens at $\langle N_{part} \rangle \sim 100$ and appears to be much weaker than at RHIC for central collisions. Such a centrality dependence and p_T differential studies suggest that the $\bar{c}c$ regeneration processes indeed play an important role at the LHC energies. The observed hint for a non-zero elliptic flow shown in Fig. 8 (right) is also in favour of this picture [10].

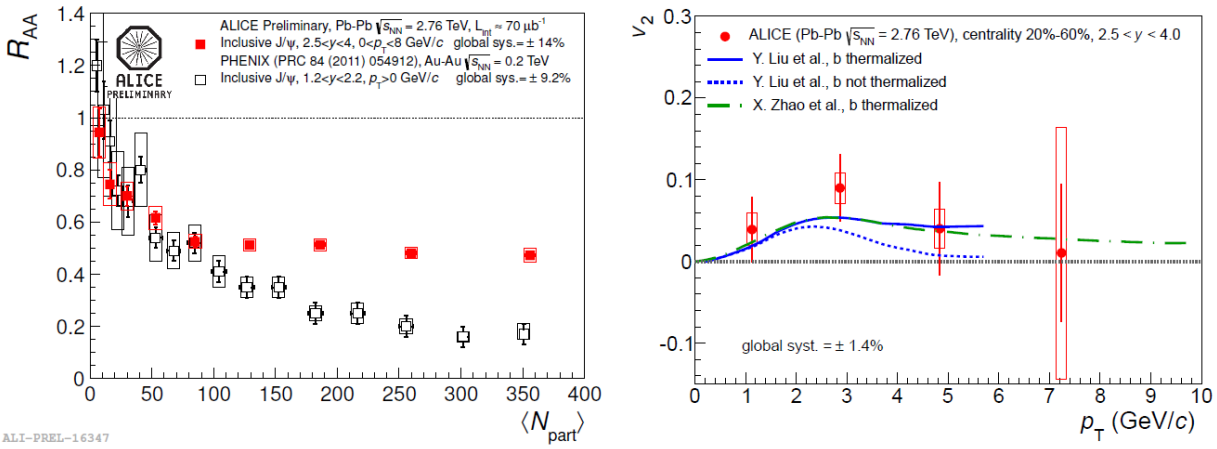

Fig. 8. Inclusive J/ψ R_{AA} as a function of the number of participants (left) and v_2 as a function of p_T (right) at the forward rapidity (from Refs. [9, 10])

7. Proton-lead results

Proton-nucleus collisions are very important for discrimination between the initial state cold nuclear matter effects in heavy ion collisions and the effects of the hot QCD matter dynamics. During a short pilot *p*-Pb run at $s_{NN}^{1/2} = 5.02$ TeV in September 2012, ALICE collected 0.9 μb^{-1} of minimum bias triggers and published first results on these data [11, 12].

Figure 9 (left) shows the pseudorapidity dependence of the charged particle density in non-single-diffractive *p*-Pb events measured by ALICE [11] in comparison with theoretical predictions. The best agreement of theory with experiment is found for the DPMJET model and HIJING2.1 with the shadowing parameter s_g tuned to describe RHIC *d*-Au data, while the gluon saturation models predict a steeper pseudorapidity dependence. The midrapidity particle density was also scaled to the number of participants and compared to few measurements at lower energies showing the trend similar to the *pp* energy dependence.

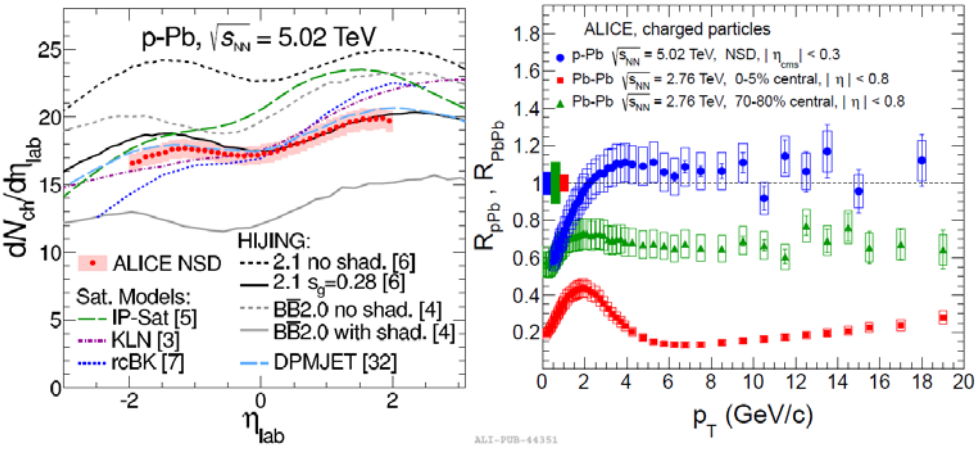

Fig. 9. Pseudorapidity density of charged particles measured in non-single-diffractive *p*-Pb collisions at $s_{NN}^{1/2} = 5.02$ TeV compared to theoretical predictions [11] (left). The nuclear modification factor in *p*-Pb and Pb-Pb collisions at the LHC [12] (right)

ALICE has also measured the nuclear modification factor R_{pPb} of charged particles as a function of the transverse momentum [12]. Figure 9 (right) presents the results in comparison to R_{AA} in central and peripheral Pb-Pb collisions measured with ALICE at $s_{\mathrm{NN}}^{1/2} = 2.76$ TeV. The observed R_{pPb} is consistent with unity at the transverse momentum above 2 GeV/c indicating that the strong suppression of hadron production measured in Pb-Pb collisions at the LHC is not an initial state effect but it is a consequence of jet quenching in the hot QCD matter.

In the beginning of 2013, ALICE collected 12 nb^{-1} of pA data allowing to make further progress in understanding of cold nuclear matter effects.

8. Study of the nuclear modification factor for neutral particles by the PNPI team

The PNPI team participates in an analysis of the data to determine the factors of nuclear modification for neutral hadrons at intermediate and high transverse momenta using the approaches developed in studies performed at RHIC. Standard particle identification techniques like measurements of the particle time-of-flight or ionization losses apparently have a very limited application in this kinematic region. Another problem is a limited statistics available for the analysis.

One of the possible solutions is a measurement of the hadron multi-particle decays with at least one gamma quantum or one neutral meson in the final state. The reconstruction of these decays benefits from the use of the high energy resolution PHOS electromagnetic calorimeter (that provides the means to measure and identify high energy photons, π^0 and eta-mesons) and online trigger selecting only events containing high energy clusters. We analysed minimum bias data samples accumulated by ALICE in 2010 for $p + p$ collisions at $s^{1/2} = 7$ TeV. So far, only a few decay channels for light hadrons such as $\omega \to \pi^0\pi^+\pi^-$, $\eta \to \pi^0\pi^+\pi^-$, $\omega \to \pi^0\gamma$, $K_s \to \pi^0\pi^0$, and $\eta' \to \eta\pi^+\pi^-$ have been considered. The choice of the particles is motivated by their large production rates at intermediate and high transverse momenta: $\omega/\pi^0 \approx 1$, $\eta/\pi^0 \approx K_s/\pi^0 \approx 0.45$, $\eta/\pi^0 \approx 0.25$. The decay modes have relatively large branching ratios: BR($\omega \to \pi^0\pi^+\pi^-$) = (89.2 ± 0.7) %, BR($\eta \to \pi^0\pi^+\pi^-$) = (22.74 ± 0.28) %, BR($\omega \to \pi^0\gamma$) = (8.28 ± 0.28) %, BR($K_s \to \pi^0\pi^0$) = (30.69 ± 0.05) %, BR($\eta' \to \eta\pi^+\pi^-$) = (43.4 ± 0.7) %. These are important considerations for the first ALICE data samples suffering from low integrated luminosities. Later, when all analysis difficulties are resolved and new high-luminosity data samples are accumulated, we will expand this study on the sector of heavy hadrons such as $D^0 \to \pi^0\pi^+K^-$ *etc*., and heavier collision systems.

Another solution is based on reconstruction of peaks in the invariant mass distribution from decay of light hadrons without identification of the daughter particles. So far, we analysed only $\phi \to K^+K^-$ decay in $p + p$ collisions at $s^{1/2} = 2.76$ and 7 TeV, p + Pb collisions at $s^{1/2} = 5.02$ TeV, and Pb + Pb collisions at $s^{1/2} = 2.76$ TeV by combining reconstructed charged tracks of opposite sign in pairs and assigning to all particles in these tracks the mass of a charged kaon. This analysis benefits from a small natural width of the ϕ-meson (Γ = 4.26 ± 0.04 MeV), large branching ratio BR($\phi \to K^+K^-$) = (48.9 ± 0.5) %, and high momentum resolution of the tracking system.

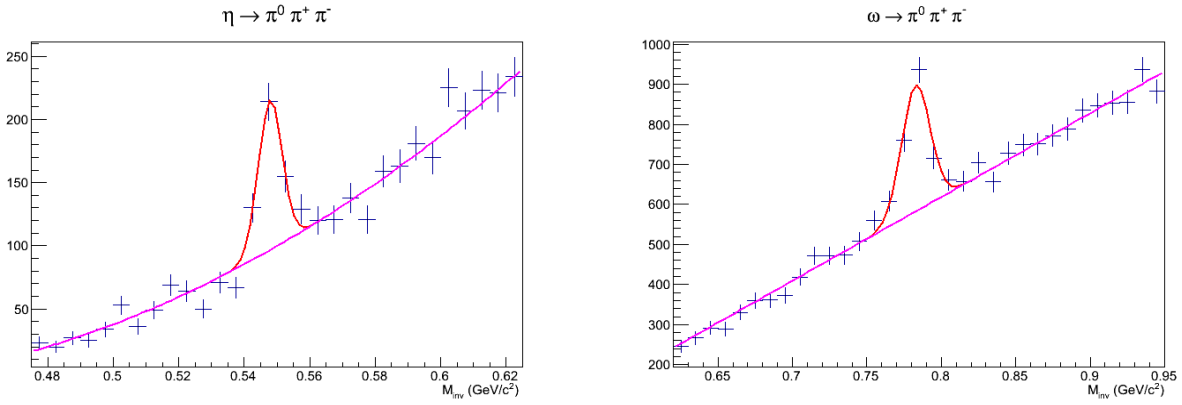

Fig. 10. Invariant mass distributions for ($\pi^0\pi^+\pi^-$) combinations

In this article, we present the results obtained by the PNPI team for light hadrons after about one year of work. The presented results are for $p + p$ collisions; they have been approved by the collaboration and can be shown in public. The remaining $p + p$ and heavy ion results of our analyses are in an advanced state, and they hopefully will be released for public next year.

Figure 10 shows an example of invariant mass distributions obtained for $(\pi^0\pi^+\pi^-)$ combinations. One can clearly see peaks from decay of η and ω mesons. The reconstructed masses of hadrons are in agreement with the PDG values. The widths of the peaks are in agreement with the values expected from simulations and equal to ~ 4 MeV/c^2 and ~ 12 MeV/c^2, respectively. Small values of the peak widths are achieved due to high energy resolution of the PHOS calorimeter and small difference in masses between the original particle and the decay products.

Figure 11a shows the invariant differential production cross section measured for the ω meson in $p + p$ collisions at $s^{1/2}$ = 7 TeV. The particle production was measured in a wide range of the transverse momentum 2–16 GeV/c. This is the first measurement in ALICE that simultaneously utilizes particle reconstruction in the calorimeter and tracking system. Figure 11b shows the ω/π ratio as a function of the transverse momentum measured in $p + p$ collisions at different energies, $s^{1/2}$ = 62–7000 GeV. This plot summarizes world-wide available measurements for the ω meson at high-p_T in $p + p$ collisions. It is interesting to note that the ratio does not depend on the collision energy within the uncertainties.

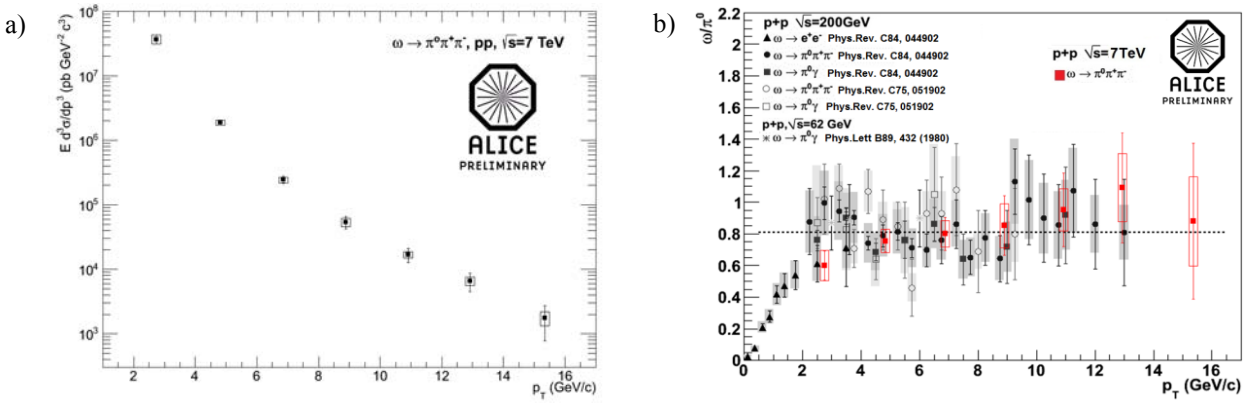

Fig. 11. a) Invariant differential production cross section measured for ω meson in $p + p$ collisions at $s^{1/2}$ = 7 TeV. b) ω/π ratio as a function of the transverse momentum measured in $p + p$ collisions at different energies, $s^{1/2}$ = 62–7000 GeV

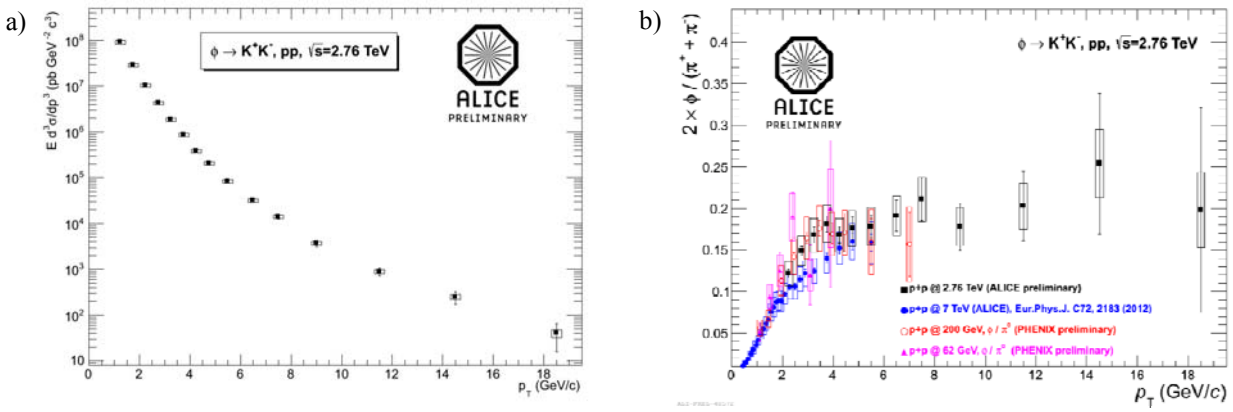

Fig. 12. a) Invariant differential yields measured for the φ meson in $p + p$ collisions at $s^{1/2}$ = 2.76 TeV. b) φ/π ratio as a function of the transverse momentum measured in $p + p$ collisions at different energies, $s^{1/2}$ = 62–7000 GeV

Figure 12a shows the invariant differential yields measured for the φ meson in $p + p$ collisions at $s^{1/2}$ = 2.76 TeV in a range of the transverse momentum 1–20 GeV/c. This is the first measurement for the φ meson at such a high momentum, previous measurements at RHIC spanning over a range

of the transverse momentum up to 7 GeV/c only. Figure 12b shows the ϕ/π ratio as a function of the transverse momentum measured in $p + p$ collisions at different energies, $s^{1/2}$ = 62–7000 GeV. As in the case of the ω meson, this ratio does not depend on the collision energy within the uncertainties.

Measurements of ω and ϕ contribute to precision tests of the pQCD at high p_T, in particular of the currently available parameterizations for fragmentation functions. The ω and ϕ mesons as vector mesons are more directly related to the partonic interactions as compared to pions or kaons, which often emerge as products of decay of more massive particles. The ω and ϕ mesons are also important components of different cocktails crucial for measurements of heavy flavor leptons and direct photons.

The results obtained in $p + p$ collisions were used to estimate the nuclear modification factors for the ϕ meson in Pb + Pb collisions at $s_{NN}^{1/2}$ = 2.76 TeV. Figure 13 shows the nuclear modification factors at different centralities measured as a function of the transverse momentum. The p_T range of the measurements is limited by the available Pb + Pb data and will be extended up to 20 GeV/c in our study. The results for ϕ are also superimposed in these plots with the factors measured for unidentified charged hadrons ($h^{\pm}$). The production of the ϕ meson at intermediate p_T-values is suppressed even in the peripheral (60–80 %) collisions. As for other light hadrons, the suppression gradually increases with the centrality and reaches the maximum in the most central (0–10 %) collisions. The production of the ϕ meson is less suppressed here than that of charged hadrons, which is similar to what was previously observed at RHIC. In the latter case, the observed effect was explained by parton recombination as a dominating particle production mechanism in this kinematic region. For further studies, it is crucial to extent the p_T range of these measurements (coming soon) and to compare the factors obtained for different identified light hadrons.

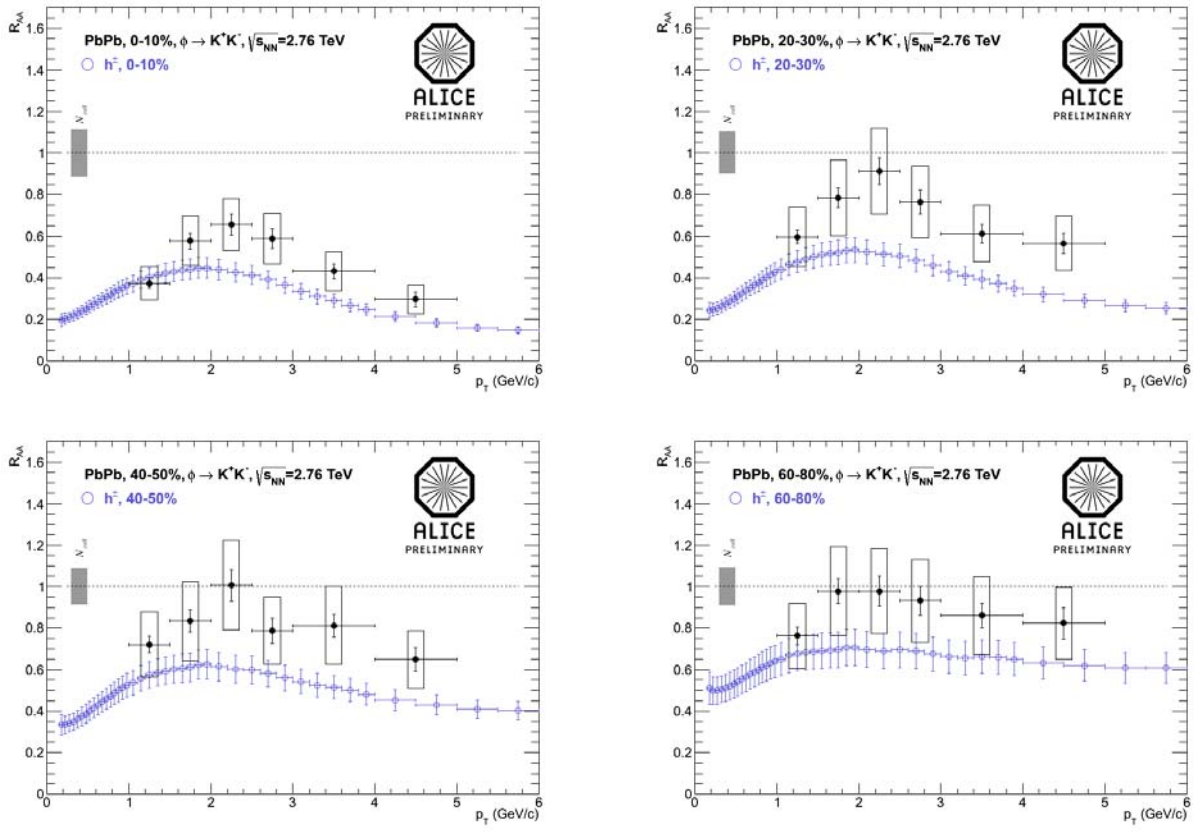

Fig. 13. Nuclear modification factors for the ϕ meson and charged hadrons as a function of the transverse momentum. Panels correspond to different centrality bins from 0–10 % (top-left) to 60–80 % (bottom-right)

9. Study of the heavy ion ultraperipheral collisions in the ALICE kinematics

From the RHIC studies it is well recognized now that the hot dense medium created in the first moment of the central collisions of heavy ions is dominated by the gluons carrying a small fraction x of the momentum of colliding nucleons. In the kinematics of RHIC, the specific values of x are of the order of 10^{-2}, and it is estimated that the nuclear gluon density $G_A(x)$ is suppressed as compared to $G_A(x) = AG_N(x)$ by a factor of about 0.8–0.9. The energy of colliding ions at the LHC is 15 times higher, hence the gluons with x in the range 10^{-3}–10^{-4} will dominate since the nucleon gluon density is known to grow as $x^{-0.2}$ with a decrease of x. The nuclear gluon density in this region of x has not been measured so far, while theoretical calculations of this quantity differ by a factor of about 3–4 due to uncertainties in the estimates of the nuclear gluon shadowing at small x in different approaches. For example, the leading twist gluon shadowing model predicts a much stronger effect than calculations in the higher twist approach. Hence, determination of $G_A(x)$ from independent measurements is a problem of key importance in a study of the properties of the QGP formed in heavy ion central collisions at the LHC.

According to the UltraPeripheral Collision (UPC) group studies, the measurements of the J/ψ photoproduction in ultraperipheral Pb + Pb collisions could be one of the most promising and clean method to obtain information on the behaviour of the nuclear gluon density at small x and to clear up the role of effects of the gluon screening in heavy nuclei since according to the perturbative QCD the cross section for this process is proportional to the squared nuclear gluon density.

During the heavy ion run in 2010–2011, the data on J/ψ coherent photoproduction in Pb + Pb UPC at 2.76 TeV were taken using a special ultraperipheral trigger. To select the ultraperipheral events, no activity other than that with the muon tracks in the TPC, FMD and V0 detectors is required. In order to estimate systematics due to noise in these detectors, a special data sample with an empty trigger was analysed. It appeared that in 0.3 % of these events the multiplicity of the FMD exceeds the threshold. As the TPC is a slow detector integrating events within ~ 0.1 ms, tracks were observed in ~ 6 % of the empty trigger events for $z > 20$ cm. All these effects were taken into account during the analysis.

The final goal of the analysis is determination of the J/ψ photoproduction cross section. So, the measured J/ψ yield should be divided by the efficiency of registration and the integral luminosity. In order to estimate the efficiency of the detector, a special event generator based on the perturbative QCD approach was developed, and simulations within the AliRoot using realistic OCDB data were performed.

The determined experimental values of the cross section for PbPb → PbPb J/ψ production were compared [13] to a number of predictions and appeared to be in better agreement with those which calculated the coherent J/ψ photoproduction on nuclear targets in the leading order (LO) pQCD taking into account the nuclear gluon shadowing. However, it is reasonable to reduce as much as possible the model dependence in comparisons of the experimental cross sections with those of different model calculations. The best strategy to achieve this goal is to analyse the ALICE results in terms of the nuclear suppression factor $S_{exp}(W_{\gamma p})$ defined as the ratio of the coherent photoproduction cross section $\sigma^{exp}{}_{\gamma Pb \to PbJ/\psi}(W_{\gamma p})$ at the given value of the centre-of-mass energy $W_{\gamma p}$ measured in the ultraperipheral ion collisions to the cross section $\sigma^{IA}{}_{\gamma Pb \to PbJ/\psi}(W_{\gamma p})$ calculated in the impulse approximation (IA), which neglects all nuclear effects except those for coherence:

$$S_{exp}(W_{\gamma p}) = [\sigma^{exp}{}_{\gamma Pb \to PbJ/\psi}(W_{\gamma p}) / \sigma^{IA}{}_{\gamma Pb \to PbJ/\psi}(W_{\gamma p})]^{1/2}.$$

Such a definition of $S_{exp}(W_{\gamma p})$ for coherent vector meson photoproduction on a nuclear target corresponds to the standard estimate of the nuclear suppression in terms of A_{eff}/A. Since the nucleus remains intact in the considered process, the transverse momentum distribution of J/ψ is dictated by the elastic nuclear form factor $F_A(t)$. Hence, the cross section in the impulse approximation can be written as

$$\sigma^{IA}{}_{\gamma Pb \to PbJ/\psi}(W_{\gamma p}) = d\sigma_{\gamma p \to pJ/\psi}(W_{\gamma p}, t = 0) / dt \int_{t_{min}}^{\infty} dt\, |F_A(t)|^2.$$

The forward differential cross section for the process $\gamma p \to pJ/\psi$ can be found from the experimental data measured at HERA, FNAL, CERN, while the nuclear form factor of Pb is well known from the studies of *e*Pb and *p*Pb elastic scattering experiments. It is important to point out that the suppression factor determined in this way is practically model independent since the estimate of the cross section in the impulse approximation is based on experimental data. This analysis was realized by the PNPI team participating in the ALICE Collaboration, and the results are compared to calculations of the suppression factors within the framework of the leading order perturbative QCD. In this theoretical approach, the nuclear suppression factor is equal to the ratio of the nuclear gluon density G_A (x, μ^2) to the gluon density in the nucleon (x is the fraction of the nucleon momentum carried by a gluon and μ^2 is the hard scale in J/ψ photoproduction):

$$S(W_{\gamma p}) = GA(x, \mu^2)/AG_N(x, \mu^2).$$

Hence, within the LO pQCD the suppression factor characterizes the nuclear gluon shadowing. The results of this analysis are published in Ref. [14] and are presented in Fig. 14.

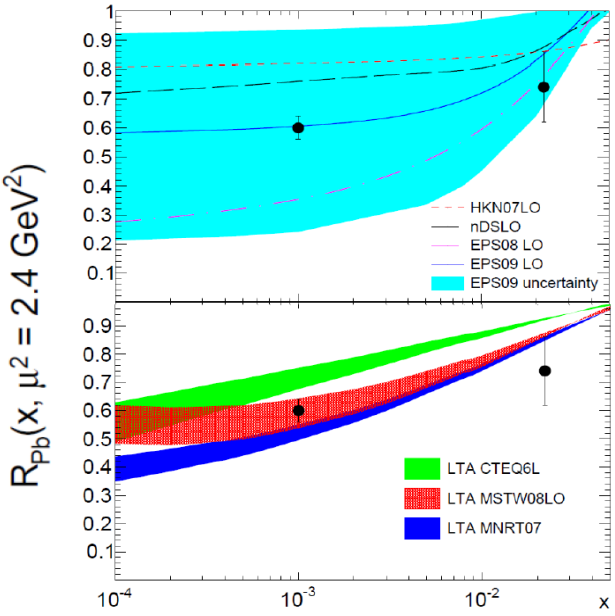

Fig. 14. Comparison of the nuclear suppression factor determined from the ALICE measurement of the coherent J/ψ photoproduction in ultraperipheral PbPb collisions at 2.76 TeV with nuclear gluon shadowing predicted in various theoretical approaches. The top panel presents a comparison with the nuclear gluon shadowing found from the Global nuclear PDF analyses of the DIS and DY processes on nuclear targets. The bottom panel compares the ALICE results to predictions of calculations of the nuclear gluon shadowing in the Leading Twist Approximation with three sets of the gluon distributions in the proton: CTEQ6L, MSTW08, and MNRT07

From a comparison of $S(W_{\gamma p})$ with $S_{exp}(W_{\gamma p})$, one finds that the ALICE measurements give the first direct experimental evidence of a rather strong nuclear gluon shadowing close to that which was obtained from the global fit nuclear parton density distribution analysis EPS09 and was predicted in the Leading Twist approximation (LTA) at small $x \sim 10^{-3}$ and at the scale 2.5–3 GeV^2.

10. Conclusion

Based on the analysis of the data collected during the 2010–2013 runs with proton-proton, proton-ion and ion-ion beams, the ALICE Collaboration has published already more than 50 papers devoted to a study of the produced extreme states of the nuclear matter. The PNPI team actively participates in all stages of this experimental study starting from the data taking during the runs up to the final data analysis. A special attention of the PNPI team in the data analysis is focused on the following two topics: the nuclear modification of the yield of particles with large transverse momenta and the investigation of the heavy quarkonium photoproduction in ultraperipheral ion collisions.

References

1. K. Aamodt *et al.* (the ALICE Collaboration), *The ALICE experiment at the CERN LHC*. JINST **3**, S08002 (2008).
2. K. Oyama for the ALICE Collaboration, *ALICE Detector status and upgrade plans*. EPJ Web Conf. **49**, 02002 (2013).
3. B. Abelev *et al*. (the ALICE Collaboration), *Upgrade of the ALICE Experiment.* The Muon Forward Tracker. CERN-LHCC-2013-**014**.
4. E. Kryshen for the ALICE Collaboration, *ALICE Status and Plans*, PoS IHEP-LHC-2012 (2012) 002.
5. K. Aamodt *et al*. (the ALICE Collaboration), *Charged-particle multiplicity density at mid-rapidity in central Pb-Pb collisions at 2.76 TeV*, Phys. Rev. Lett. **105**, 252301 (2010).
6. K. Aamodt *et al*. (the ALICE Collaboration), *Elliptic flow of charged particles in Pb-Pb collisions at 2.76 TeV*, Phys. Rev. Lett. **105**, 252302 (2010).
7. K. Aamodt *et al*. (the ALICE Collaboration), *Suppression of charged particle production at large transverse momentum in central PbPb Collisions at 2.76 TeV*, Phys. Lett. B **696**, 30 (2011).
8. B. Abelev *et al*. (the ALICE Collaboration), *Suppression of high transverse momentum D mesons in central Pb-Pb collisions at 2.76 TeV*, JHEP **1209**, 112 (2012).
9. B. Abelev *et al*. (the ALICE Collaboration), *J/ψ suppression at forward rapidity in Pb-Pb collisions at 2.76 TeV*. Phys. Rev. Lett. **109**, 072301 (2012).
10. E. Abbas *et al*. (the ALICE Collaboration), *J/ψ elliptic flow in Pb-Pb collisions at 2.76 TeV*. arXiv:1303.5880 [nucl-ex].
11. B. Abelev *et al*. (the ALICE Collaboration), *Pseudorapidity density of charged particles in p-Pb collisions at 5.02 TeV*, Phys. Rev. Lett. **110**, 032301 (2013).
12. B. Abelev *et al*. (the ALICE Collaboration), *Transverse momentum distribution and nuclear modification factor of charged particles in p-Pb collisions at 5.02 TeV*, Phys. Rev. Lett. 110, 082302 (2013).
13. E.Abbas *et.al.* (the ALICE Collaboration), *Charmonium and e^+e^- pair photoproduction at midrapidity in ultraperipheral PbPb collisions at 2.76 TeV*, arXiv:1305.1467 [hep-ex], 2013.
14. V. Guzey, E. Kryshen, M. Strikman, M. Zhalov, *Evidence for nuclear gluon shadowing from the ALICE measurements of PbPb ultraperipheral exclusive J/ψ production*, Phys. Lett. B **726**, 290 (2013).